Investigation on the Decomposition Enthalpy of Novel Mixed Mg(1–x)Znx(BH4)2Borohydrides by Means of Periodic DFT Calculations

(Article begins on next page)

18 October 2024

iris-AperTO

Investigation on the Decomposition Enthalpy of Novel Mixed $Mg_{(1-x)}Zn_x(BH_4)_2$ Borohydrides by means of periodic DFT calculations

Elisa Albanese, Bartolomeo Civalleri,[*] Silvia Casassa, and Marcello Baricco

Dipartimento di Chimica e Centro Interdipartimentale NIS, Università di Torino, Via P. Giuria 7 10125 Torino (Italy)

E-mail: bartolomeo.civalleri@unito.it

---

[*]To whom correspondence should be addressed

Abstract

The combination of $Mg(BH_4)_2$ and $Zn(BH_4)_2$ compounds has been theoretically investigated as a possible mixed borohydride prone to give an enthalpy of decomposition around 30 kJ/mol_{H_2}, i.e. suitable for a dehydrogenation process close to room temperature and pressure. The total energy of pure compounds and solid solutions has been computed by means of periodic DFT calculations. To generate the $Mg_{(1-x)}Zn_x(BH_4)_2$ solid solutions, the α-phase of $Mg(BH_4)_2$ (space group $P6_122$) has been considered in which Mg^{2+} ions have been progressively replaced with Zn^{2+}, without lowering the symmetry of the crystalline structure. A charge density topological analysis is reported to better understand the chemical bonding in the pure and mixed metal borohydrides. The decomposition enthalpy of the mixed borohydrides according to two different reaction paths that lead to MgH_2, Zn, H_2 and α-B or B_2H_6, respectively, as products has been estimated. As regards the former, a value of about 30 kJ/mol_{H_2} has been predicted for a $Mg_{(1-x)}Zn_x(BH_4)_2$ solid solution with x=0.2-0.3.

Introduction

Hydrogen is a potential, extremely interesting energy carrier,[1] but a major challenge in a future "hydrogen economy" is the development of a safe and efficient way to store it, in particular for mobile applications.[2] Among others, solid state hydrogen storage is considered as a possible solution. In fact, the use of hydrogen storage materials for technical applications, requires high H_2 gravimetric density and thermodynamic and kinetic properties that allows the hydrogen release around room temperature and pressure. In addition, fast sorption kinetics, high cyclability and low cost are desirable. For the decomposition enthalpy, ΔH_{dec},

a target value around $\approx$ 30 kJ/mol$_{H_2}$ is expected[3,4], even if, so far, no single material has yet been found that fulfills all criteria for hydrogen storage.

Metal Borohydrides (MBHs), in particular light-metal borohydrides, have attracted great interest because of their high hydrogen-storage capacities. For instance, they show a gravimetric content of hydrogen up to 20.8% (for $Be(BH_4)_2$) but, unfortunately, most of them are either thermodynamically too stable or kinetically too slow. On the other hand, heavy-metal BHs can be metastable, with hydrogen sorption reactions practically irreversible.[5]

Substitution of metal ions or BH_4 groups by other cations and anions, respectively, provides a general route to destabilize light-metal borohydrides and for tuning their thermodynamic stability.[6] Therefore, current research is seeking for new mixed MBHs and several mixed-anion[7–11] and -cation[12–17] compounds have been studied, both theoretically and experimentally.

As regards the cation substitution, among the new mixed MBHs, the series of alkali-zinc borohydrides, such as $MZn_2(BH_4)_5$ (M = Li, Na) and $NaZn(BH_4)_3$ have been suggested. They show two new types of structures, different from known inorganic compounds as confirmed by synchrotron radiation powder X-ray diffraction.[18] It was pointed out that they show a significant structural diversity and room decomposition temperatures that may be assigned to the instability of the pure $Zn(BH_4)_2$. Although it has not yet been isolated in its free form and its structure is still unknown - only an hypothetical structure has been proposed on the basis of a a theoretical crystal structure prediction analysis[19] - it likely decomposes at low temperature, thus destabilizing MBHs. Interestingly, a linear correlation between Pauling electronegativites of the cation and decomposition temperatures of MBHs has been found.[20] Therefore, the higher Pauling electronegativity of zinc than alkali metals can be one of the reason for the reduced stability of Zn-containing borohydrides. The variation in the ratio between the alkali and the transition metal, as well as the use of different metals, enables, in turn, the tuning of the hydrogen desorption properties in alkali metal-transition metal-BH_4 systems.

Here, we investigate the $Zn(BH_4)_2$ as a possible candidate to be mixed with a light-metal borohydride compound with a divalent cation. To identify a dual-cation MBH with a suitable ΔH_{dec}, a first screening of possible candidates was performed on the basis of available data.[15,18,21] In particular, we re-analyzed theoretical results of ΔH_{dec} obtained by Vegge and co-workers[21] on a large set of mixed borohydrides with alkali metals. We found out that the decomposition enthalpies of the mixed MBHs computed in Ref.[21] could be compared to a simple averaging of the corresponding ΔH_{dec} of the pure MBHs if an ideal solid solution was considered (see Supporting Information for further details, Figure S1 and S2). By applying this simple scheme to divalent MBHs, we recognised that $Mg(BH_4)_2$ - one of the most promising MBHs for hydrogen storage because of its high gravimetric hydrogen content (14.9 mass% hydrogen) - appeared to be a suitable candidate to be mixed with $Zn(BH_4)_2$. In fact, Vegge and co-workers[21] computed a decomposition enthalpy for pure Mg and Zn BH of 45 kJ/mol_{H_2} and 6 kJ/mol_{H_2}, respectively. It turns out that an average decomposition enthalpy not far from the target value of 30 kJ/mol_{H_2} is predicted for a hypothetical $Mg_{0.5}Zn_{0.5}(BH_4)_2$ mixed compound. In addition, it is expected that the formation of the mixed compound could be favored because Zn^{2+} has a similar ionic radius and comparable electronegativity with respect to Mg^{2+}.

It is worthy to mention that our theoretical investigation on the $Mg_{(1-x)}Zn_x(BH_4)_2$ systems was performed in parallel with the synthesis and experimental characterization of a real mixed Mg/Zn borohydrides[22,23]. In summary, the experimental work shows that: (i) at ambient conditions, the mixing between $Mg(BH_4)_2$ and $ZnCl_2$ is spontaneous; (ii) mixed Mg/Zn compounds were successfully synthesized with different amount of Zn; (iii) these do not show the formation of a new phase and (iii) for x=0.06-0.1 the H_2 release begins approximately at 125 °C, thus showing a significant decrease in the decomposition temperature compared to the pure $Mg(BH_4)_2$. In addition, a very small release of impurity gases, i.e. B_2H_6, has also been observed during the decomposition.

In the present work, we report full details of the theoretical investigation of mixed Mg/Zn borohydrides by means of periodic DFT calculations. By considering the experimental evidences that do not report the formation of a new structure Mg/Zn,[23] we designed the $Mg_xZn_{1-x}(BH_4)_2$ solid solutions starting from the α-phase of $Mg(BH_4)_2$.

The structure of the paper is as follows. In the next section, we concisely illustrate the theoretical methods used for the calculations and other computational details. In the "Results and discussion" section, we report the main outcomes of the present work by discussing: (i) the models and the structural features of the mixed MBHs, (ii) the charge density topological analysis of the M^{2+}–$[BH_4]^-$ bond of the pure MBHs and of the most promising mixed Mg/Zn solid solution, (iii) the enthalpies of formation of the mixed Mg/Zn BHs and (iv) the ΔH_{dec} of two possible decomposition paths.

Computational Details

The investigation of mixed MBHs was carried out with periodic density functional theory (DFT) calculations employing the PBE[24] functional as implemented in the CRYSTAL program.[25,26] Crystalline orbitals are represented as linear combinations of Bloch functions (BF) and are evaluated over a regular three-dimensions mesh of points in reciprocal space. Each BF is built from local atomic orbitals (AO) which are contractions (linear combinations with constant coefficients) of Gaussian-type-functions which in turn are the product of a Gaussian times a real solid spherical harmonic function. All electron basis sets have been used for all the atoms. The best compromise between computation time and accuracy was determined and it consists of a triple-ζ valence plus polarization (TZVP) basis set for Zn^{27}, a 6-311G* for Mg and a 6-31G* for H and B (the first figure refers to an s shell, the others to sp and d shell contractions, respectively). For the numerical integration of exchange-correlation term, 75 radial points and 974 angular points (XLGRID) in a Lebedev scheme in the region of chemical interest were adopted. The Pack-Monkhorst/Gilat shrinking factors for the reciprocal

space were set to 6, corresponding to 28 real reciprocal space points at which the Hamiltonian matrix was diagonalized. The accuracy of the integral calculations was increased with respect to its default value by setting the tolerances to 7, 7, 7, 7 18. The self-consistent field (SCF) iterative procedure has been converged to a tolerance in total energy of $\Delta E = 1 \cdot 10^{-7}$ a.u.. The above computational parameters ensured a full numerical convergence on all the computed properties described in this work.

Vibrational frequencies at the Γ point were calculated to estimate the thermodynamic properties. The normal modes were calculated on the optimized geometry by means of a mass-weighed Hessian matrix, obtained by numerical differentiation of the analytical first derivatives.[28,29]

In order to compute an enthalpy of mixing, reaction and decomposition (see Eqs. (3) to (5)) at $T = 298.15$ K and $p = 1$ atm, the computed electronic energy E_{el} has been corrected for the zero point energy (E_{ZPE}), the thermal correction to enthalpy ($E_T(T)$) necessary to heat the system from 0 K to T and the $P \cdot V$ (pressure $\cdot$ volume) contribution. The latter is negligible for solids at room pressure, while it corresponds to RT for molecules when considered to behave as an ideal gas. The enthalpy is then obtained as:

$$H(T) = E_{el} + E_{ZPE} + E_T(T) \tag{1}$$

These thermodynamic functions can be obtained by summing the contribution of the vibrational modes at various points of the first Brillouin zone. In the present work, due to the large size of the unit cell of the α-Mg(BH$_4$)$_2$ (lattice parameters are a=10.17 Å and c=36.33 Å) only the Γ point has been considered in the sum (i.e. phonon dispersion has been neglected). As regards the other solids involved in the formation and decomposition reactions, i.e. MgCl$_2$, ZnCl$_2$, MgH$_2$, α-Boron and Zn, supercells with appropriate size were built in order to allow for phonon dispersion. Structural information and other computational details are reported in Table S1 in the Supporting Information.

An updated version of the program TOPOND,[30,31] as encoded into the new version of the CRYSTAL code, was employed to perform the charge density topological analysis, according to the Quantum Theory of Atoms In Molecules originally proposed for molecules by Bader[32] and subsequently extended to crystals (QTAIMAC) .[33]

Results and Discussion

Mixed Mg/Zn Borohydrides: Models and Structural Features

To generate the $Mg_{(1-x)}Zn_x(BH_4)_2$ solid solution, the starting point was the most stable phase of $Mg(BH_4)_2$ at room temperature, i.e. the α-phase, whose Mg^{2+} cations were replaced with Zn^{2+}. The α-phase shows a hexagonal lattice (space group $P6_122$) with 330 atoms in the unit cell. It contains three symmetrically independent Mg^{2+} and $[BH_4]^-$ ions connected into a three dimensional framework (Figure 1). All Mg^{2+} ions have similar atomic environments being surrounded by four $[BH_4]^-$ ions arranged in a deformed tetrahedron. Each $[BH_4]^-$ ion is approximately linearly coordinated by two Mg^{2+} ions. The orientation of the $[BH_4]^-$ ions is such that each Mg^{2+} ion is coordinated by tetrahedral edges only, resulting in an unusual eightfold, relatively irregular hydrogen coordination environment.[34-36]

Due to the computational burden of dealing with such a large number of atoms per unit cell and the number of possible substitution sites (i.e. 30), we only explored the solid solutions that do not lower the symmetry of the crystalline structure. By replacing, in turn, the three Mg^{2+} ions not equivalent by symmetry, we obtained six mixed $Mg_{(1-x)}Zn_x(BH_4)_2$ compounds with the following molar fraction of zinc: $x = 0.2, 0.4, 0.6$ and 0.8 (see Table1). For $x=0.2$ and $x=0.8$, just one Mg^{2+} ion was replaced by Zn^{2+}, while for $x=0.4$ and 0.6, two different configurations were generated. Eventually, six mixed Mg/Zn solid solutions were considered.

The substitution of Mg^{2+} with Zn^{2+} leads to significant lattice distortions, as a consequence of the structural changes around the substituted ion. Calculated cell parameters and volumes of the $Mg_{(1-x)}Zn_x(BH_4)_2$ solid solutions are reported in Table 2. The increase of the

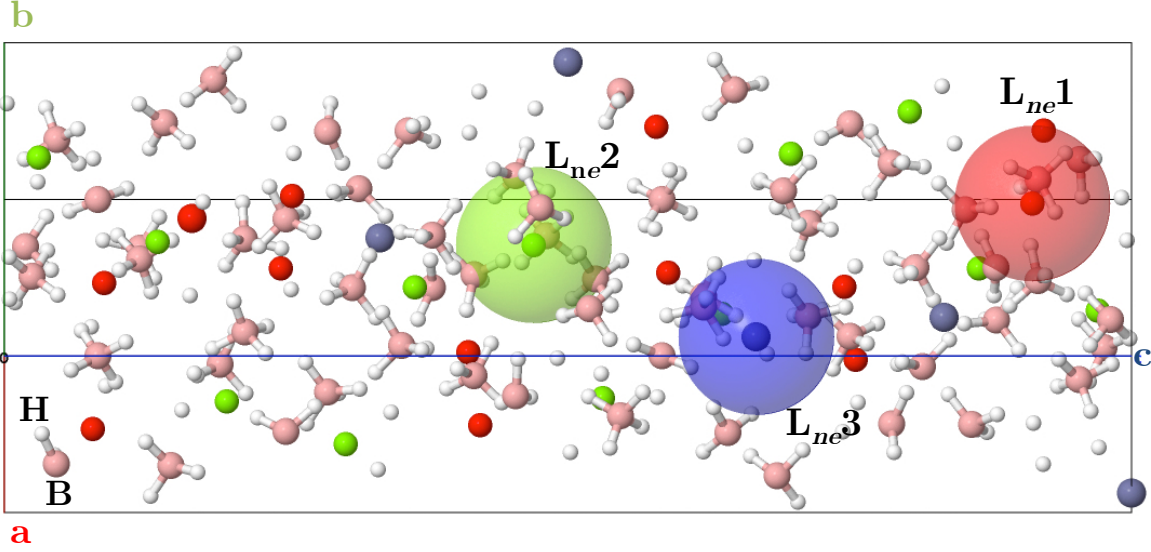Figure 1: Unit cell of the α-phase of $Mg(BH_4)_2$. Mg in position $L_{ne}=1$ are in red, $L_{ne}=2$ in green and $L_{ne}=3$ in blue. B and H are depicted in pink and white, respectively. The cell axis are reported.

Table 1: Label of non-equivalent cations in the unit cell (L_{ne}) and number of cations symmetry related to each L_{ne} (N_{eq}). For each compound the atomic species (i.e. Mg or Zn) that occupies those positions is reported.

L_{ne}	1	2	3
Site Molteplicity (N_{eq})	12	12	6
$Mg(BH_4)_2$	Mg	Mg	Mg
$Mg_{0.8}Zn_{0.2}(BH_4)_2$	Mg	Mg	Zn
a-$Mg_{0.6}Zn_{0.4}(BH_4)_2$	Mg	Zn	Mg
b-$Mg_{0.6}Zn_{0.4}(BH_4)_2$	Zn	Mg	Mg
a-$Mg_{0.4}Zn_{0.6}(BH_4)_2$	Mg	Zn	Zn
b-$Mg_{0.4}Zn_{0.6}(BH_4)_2$	Zn	Mg	Zn
$Mg_{0.2}Zn_{0.8}(BH_4)_2$	Zn	Zn	Mg
$Zn(BH_4)_2$	Zn	Zn	Zn

amount of Zn into α-Mg(BH$_4$)$_2$ causes a contraction of the volume cell, with an almost linear trend as a function of composition. This behavior, that has been confirmed by the XPD patterns,[23] can be related to a stronger covalent character of the chemical bond between the Zn^{2+} and the two H of the [BH$_4$]$^-$ ion directed towards it. The average bond lengths of Mg(BH$_4$)$_2$, Zn(BH$_4$)$_2$ and mixed compounds are reported in Table 3. In the case of pure Zn(BH$_4$)$_2$, the distance between the cation and the [BH$_4$]$^-$ ion shows a relevant shortening with respect to the Mg(BH$_4$)$_2$, with a percentage difference ($\Delta\%$) of about -2.1% and -3.2% for the M–H and M–B distances, respectively. For the Mg$_{(1-x)}$Zn$_x$(BH$_4$)$_2$ mixed systems, the $\Delta\%$ values show that each M^{2+}–[BH$_4$]$^-$ unit, i.e. Mg^{2+}–[BH$_4$]$^-$ and Zn^{2+}–[BH$_4$]$^-$, do not undergo relevant changes with respect to those of the pure MBHs upon the formation of the mixed compound. The average variation of the bond lengths with respect to the corresponding pure MBH is, indeed, always lower than 1% (see Table S2 in the Supporting Information for details) while the B–H distance appears not to be significantly influenced by the cation substitution. The replacement with Zn^{2+} ions affects only the cation-anion distance, but not the coordination, as discussed later in more detail. This tendency of Zn^{2+} of preserving a tetrahedral coordination in the case of mixed-cation BHs was already shown for NaZn(BH$_4$)$_3$[18] and also predicted by Łodziana and van Setten[37] on the basis of the relation between bonding and the structure of MBHs. Overall, the presence of Zn^{2+} in the structure of α-phase leads mainly to a shortening of the M–B bond length and then to the linear volume contraction.

Charge density topological analysis of the M^{2+}–[BH$_4$]$^-$ bond

The nature of the M^{2+}–[BH$_4$]$^-$ bond (M=Mg,Zn) in MBHs is still a matter of debate. It was recently investigated and speculated by Filinchuk et al.[38] that the directionality of the Mg–(BH$_4$)–Mg fragment and the relatively small charge transfer from Mg^{2+} to [BH$_4$]$^-$ is an evidence of a partly covalent character of the bond. They suggested a comparison of the bonding in metal borohydrides with the one between metal and linkers in metal organic

9

Table 2: Cell parameters (a and b in Å) and volume (Å^3) of $Mg(BH_4)_2$, $Zn(BH_4)_2$ and the mixed compounds $Mg_{(1-x)}Zn_x(BH_4)_2$ for all the molar fractions of Zn. The percentage differences $\Delta\%$ are computed with respect to the $Mg(BH_4)_2$.

	a	c	volume	$\Delta\%$
$Mg(BH_4)_2$	10.168	36.330	3252.5	0.0
$Mg_{0.8}Zn_{0.2}(BH_4)_2$	10.049	36.197	3165.6	-2.7
a-$Mg_{0.6}Zn_{0.4}(BH_4)_2$	10.127	35.855	3184.2	-2.1
b-$Mg_{0.6}Zn_{0.4}(BH_4)_2$	10.048	35.646	3117.0	-4.2
a-$Mg_{0.4}Zn_{0.6}(BH_4)_2$	10.017	35.755	3107.1	-4.4
b-$Mg_{0.4}Zn_{0.6}(BH_4)_2$	9.927	35.556	3034.5	-6.7
$Mg_{0.2}Zn_{0.8}(BH_4)_2$	9.980	35.283	3043.6	-6.4
$Zn(BH_4)_2$	9.873	35.189	2970.4	-8.7

Table 3: Average bond length (Å) of $Mg(BH_4)_2$ and $Zn(BH_4)_2$. Listed bonds refer to the first nearest neighbors to the metal. Percentage differences ($\Delta\%$) are computed with respect to $Mg(BH_4)_2$.

	M–H	M–B	B–H
$Mg(BH_4)_2$	2.036	2.367	1.231
$Zn(BH_4)_2$	1.993	2.301	1.231
$\Delta\%$ (Zn *vs* Mg)	-2.1	-3.2	0.0

frameworks. In our opinion, despite the ascertained directionality of the Mg^{2+}–$[BH_4]^-$ interaction, this comparison with the mostly covalent bonds in metal organic frameworks is not justified. This motivated us to investigate the nature of the M^{2+}–$[BH_4]^-$ bond and to obtain information about the effect of cation substitution on it. To this purpose, a detailed topological analysis of the charge density in $Mg(BH_4)_2$ and $Zn(BH_4)_2$ has been performed by using the language of QTAIMAC.[32,33] In addition, we focused on the $Mg_{0.8}Zn_{0.2}(BH_4)_2$ mixed composition, because it resulted to be the most promising one for its decomposition enthalpy close to the target value (*vide infra*).

The most relevant QTAIMAC observable quantities for the present analysis are gathered in Table 4. Before discussing the details of the current results, we briefly recall the meaning of the QTAIMAC derived parameters we used to analyze the chemical bonding. The simplest and easiest proposed bond classification is based on the sign of the Laplacian of the electron density computed at the bond critical point (bcp). The critical points are the positions where the gradient of the electron density, $\nabla\rho$, vanishes. There are four types of cp denoted as (3,-3), (3,-1), (3,+1) and (3,+3), where the two digits are the number of nonzero eigenvalues of the Hessian matrix (i.e. the curvature of $\rho(\mathrm{r})$) and the sum of their signs, respectively.[32,33] Each type of cp may be put in one to one correspondence with a "chemically" recognizable elements in crystal: (3,-3) identify nuclei, (3,-1) bonds, (3,+1) rings and (3,+3) cages. For our purpose, we focus on the bcp (3,-1), that are characterized by two negative curvatures of $\rho(\mathrm{r}_{bcp})$ measured in two directions perpendicular to the bond path, $|\lambda_1|$ and $|\lambda_2|$, and a positive curvature along the bond path, $|\lambda_3|$, thus representing a saddle point in the electronic density distribution.

Generally, negative values of $\nabla^2\rho$ at the bcp reflect a local concentration of charge, with electron charge being accumulated toward the atomic interaction line, and imply a shared chemical interactions, i.e. pure and polar covalent bonds. Conversely, positive values reveal a local depletion of the charge and characterize closed shell interaction, such as ionic bond and van der Waals interactions. The Laplacian is related to the electronic energy density

11

$H(r)$ (i.e. $H(r) = G(r) + V(r)$) through the local expression of the virial theorem:

$$\frac{1}{4}\nabla^2\rho(r) = 2G(r) + V(r) = G(r) + H(r) \tag{2}$$

where $G(r)$ is the positive definite kinetic energy density and $V(r)$ the potential energy density. Since $G(r)$ is positive everywhere and $V(r)$ is negative everywhere, the virial theorem states that the sign of the Laplacian determines which of these two contributes is in local excess. A closed-shell interaction will thus be locally dominated by the kinetic energy, while a shared interaction is locally dominated by the potential energy at the bcp. As reported

Table 4: **Bond critical points (bcp) in the electron density. The reported values are the average of the data related to all bond critical points. ρ is the electron density, $\nabla^2\rho$ is the Laplacian, G is the positive kinetic energy density evaluated at the bcp, V is the potential energy density and H is the sum of G and V term. H/ρ defines the bond degree (BD) parameter. All the data are expressed in a.u..**

System	Bond	ρ	$\nabla^2\rho$	$|V|/G$	H/ρ
$Mg(BH_4)_2$	Mg–H	0.029	0.105	1.007	-0.006
	B–H	0.153	-0.175	2.421	-0.963
$Zn(BH_4)_2$	Zn–H	0.052	0.125	1.234	-0.184
	B–H	0.153	-0.183	2.454	-0.957
$Mg_{0.8}Zn_{0.2}(BH_4)_2$	Mg–H	0.029	0.107	1.003	-0.003
	Zn–H	0.049	0.116	1.224	-0.171
	B–H	0.153	-0.176	2.428	-0.962

in Table 4, the average values of $\nabla^2\rho$ computed at each bcp of the M–H and B–H bonds for the three systems confirm the covalent nature of the latter and reveal a closed shell interaction for the M–H bonds. With the simple analysis of the sign of the Laplacian nor other observations on the nature of the M–H bonds neither a comparison between the two different cations can be done. A better understanding of the bond nature can be obtained by considering the classification based on the adimensional $|V|/G$ ratio proposed by Espinosa et al.[39] By analyzing the $|V|/G$ ratio, they identified three characteristics bonding regime:

(i) a pure closed-shell interaction region characterized by $|V|/G < 1$ and hence positive $\nabla^2\rho$; (ii) a pure shared-shell interaction region, with $|V|/G > 2$ and negative $\nabla^2\rho$; and (iii) an intermediate transit region, with the $|V|/G$ ratio between 1 and 2, implying positive Laplacian values. This classification has been performed on the H–F bond, but it has also been successfully used for metal-metal interaction studies.[40] Furthermore, Espinosa et al.[39] defined a bond degree (BD) parameter, that expresses the total energy per electron at the bcp: $H(r)/\rho$. The BD is negative inside the shared-shell and transition region, and the greater its magnitude, the more covalent and stronger the bond. Conversely, the BD is positive in the closed shell region. The differences between the Mg–H and Zn–H bonds have been analyzed on the basis of these chemical bonding indicators. The two metal-hydrogen interactions show a slightly different nature. With a negative BD value and $|V|/G$ between 1 and 2, they reveal to belong to the intermediate transit region, but in the $Mg(BH_4)_2$ the M–H bond shows a stronger ionic character, BD = -0.006 and $|V|/G = 1.007$ (see Table 4), with respect to the $Zn(BH_4)_2$ (BD = -0.187 and $|V|/G = 1.234$). Therefore, the Zn–H interatomic contact shows a more pronounced covalent character than Mg–H. These results confirm that the latter can not be considered as a pure closed-shell bond. To further highlight the difference between the two M–H bonds, the deformation densities are reported in Figure 2 as the difference between the electron density in the crystal and as a superposition of non-interacting atomic densities. The stronger covalent character of the Zn–H bond in the $Zn(BH_4)_2$ is clearly visible. The charge density of the valence shell of the Zn ion (see Figure 2 on the right) appears to be deformed and elongated towards the H atoms (H on the same plane, i.e. H1 and H2, see Fig. 2) and then indicates a highly directional bonds. Conversely, in the case of $Mg(BH_4)_2$, the valence shell charge density is symmetrically deformed and does not evidence any preference towards the hydrogen atoms, but interacts with the entire $[BH_4]^-$ ion.

Notably, results in Table 4 show that, in the $Mg_{0.8}Zn_{0.2}(BH_4)_2$ solid solution, the QTAIMAC indicators do not change significantly upon the substitution of Mg with Zn. This implies
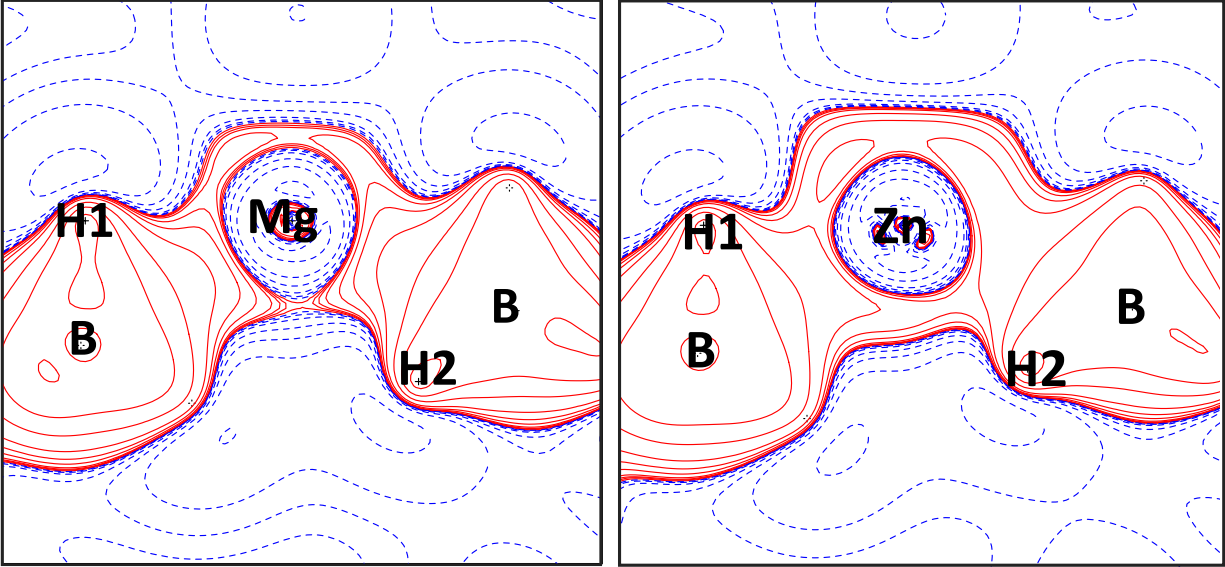
Figure 2: Difference between the charge density of the interacting crystal and the charge density obtained as superposition of atomic densities for $Mg(BH_4)_2$ (left) and $Zn(BH_4)_2$ (right). The H1, M and H2 lie on the same plane.

that the cation exchange in the α-$Mg(BH_4)_2$ structure does not perturb the chemical bonding around magnesium to a large extent. This is an interesting aspect that can have important consequences on the enthalpy of mixing between the two MBHs, as will be discussed in the next section.

Formation of the Mixed Mg/Zn Borohydrides

The enthalpy of mixing at room temperature (RT) for Mg/Zn borohydrides have been calculated according to:

$$(1-x)Mg(BH_4)_2 + xZn(BH_4)_2 \rightarrow Mg_{(1-x)}Zn_x(BH_4)_2 \tag{3}$$
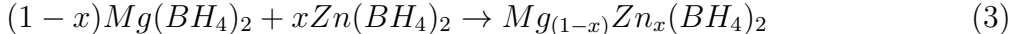
In Figure 3, the results show that the values for all the different x compositions are extremely small, i.e. the maximum ΔH_{mix} absolute value does not exceed 1.0 kJ/mol. If we take into account the possible sources of errors in the computational strategy adopted (e.g. basis set dependence, level of theory, etc.) an error bar of $\approx$1.5 kJ/mol can be estimated,

thus yielding a net enthalpy of mixing close to zero for all the Mg/Zn compositions. Such ΔH_{mix} values suggest an ideal trend when mixing the two pure borohydrides. It turns out that the substitution of Mg^{2+} with Zn^{2+} does not imply neither a loss nor a gain in the enthalpy. This behavior can be explained on the basis of the topological analysis of the charge density as reported in the previous section. In fact, the ionic character of the $Mg^{2+}-$ $[BH_4]^-$ bond is not perturbed by the presence of Zn or, viceversa, the more covalent nature of the $Zn^{2+}-[BH_4]^-$ bond is unaltered by Mg (see results for x=0.2 in Table 4).
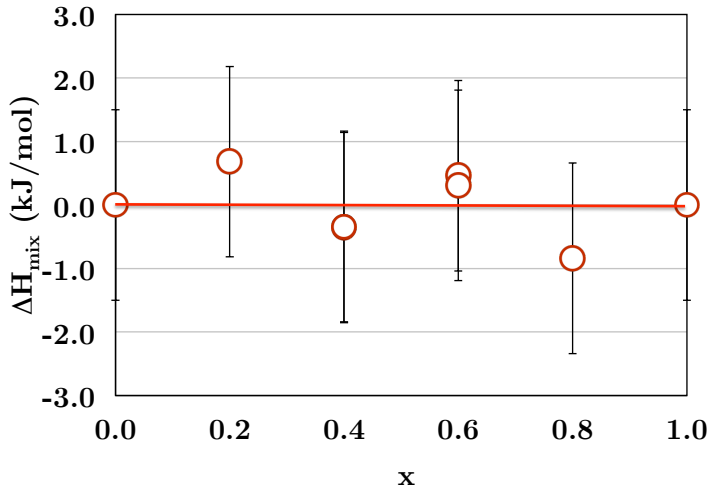

Figure 3: Enthalpy of mixing at room temperature of $Mg_{(1-x)}Zn_x(BH_4)_2$ for reaction in Eq.3. The error bars represent the estimated error of the computational method ($\approx \pm 1.5$ kJ/mol, see text). The red line indicates the mixing enthalpy equal to zero.

In addition, we can estimate the free energy of mixing for each mixed metal compound by including the configurational entropy as entropy of mixing for an ideal solution (i.e. $\Delta S_{mix} = -R(xlnx + (1-x)ln(1-x))$, vibrational entropy is negligible). In Figure 4, the corresponding ΔG_{mix} values are plotted as a function of temperature for each molar fraction. Note that enthalpy and configurational entropy of reaction are considered independent from temperature in the range 0-400 K and then maintained fixed for each temperature. It appears that the reaction may occur spontaneously above room temperature for all compositions. As a further step, we investigated the formation of the mixed Mg/Zn BHs through the
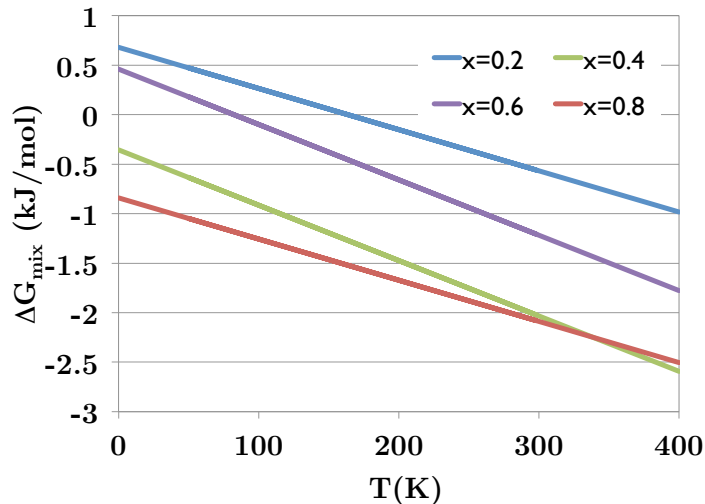
Figure 4: Free energy of mixing for reaction in Eq.3 plotted as a function of temperature for each molar fraction. The colored lines represent the molar fraction of zinc (x): blue x=0.2, green x=0.4, violet x=0.6 and red x=0.8. For x=0.2 and 0.4 the two configurations show a very similar trend. For this reason only one configuration (a) is reported.

reaction of $Mg(BH_4)_2$ and zinc chloride. Such reaction is usually employed for the synthesis of borohydrides[18] and it was used to synthesize mixed Mg/Zn BHs.[22,23]

$$Mg(BH_4)_2 + xZnCl_2 \rightarrow Mg_{(1-x)}Zn_x(BH_4)_2 + xMgCl_2 \tag{4}$$
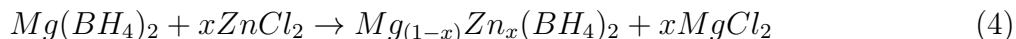
The predicted enthalpies of reaction as a function of the molar fraction of Zn in the solid solution are reported in Figure 5. A linear correlation is observed, i.e. the ΔH becomes more negative when the amount of zinc in the mixed compounds decreases. The presence of $ZnCl_2$ leads to the formation of $MgCl_2$, which is the driving force of the reaction. The formation of $MgCl_2$ is, indeed, strongly exothermic, its ΔH°_{for} is -641.8 kJ/mol (at 298 K and 1 atm)[41] and then strongly promotes the synthesis of the Mg/Zn BHs. In the limit case of x=1, the complete conversion of $Mg(BH_4)_2$ to $Zn(BH_4)_2$ is attained with a value of $\Delta H_{reac} = $ -13 kJ/mol. This trend suggests that, without a proper dosage of the zinc chloride during the synthesis, the reaction would evolve to the complete formation of $MgCl_2$, without formation of solid solution.
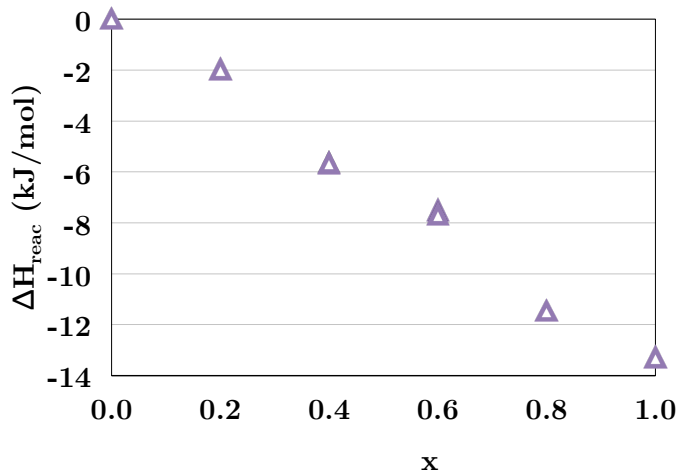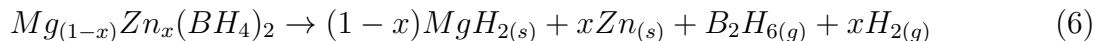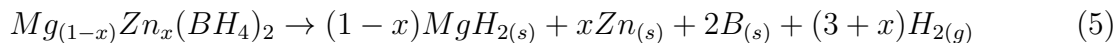
Figure 5: Enthalpy of reaction at room temperature of $Mg_{(1-x)}Zn_x(BH_4)_2$ for Eq. 4.

Decomposition of $Mg_{(1-x)}Zn_x(BH_4)_2$ solid solutions

The decomposition of $Mg(BH_4)_2$ was recently proposed to proceed in several steps, including the formation of MgH_2 and of complex B_xH_y species.[5,42–45] For the $Zn(BH_4)_2$, even if unstable at RT, it has been hypothesized that it decomposes to metallic Zn, diborane B_2H_6, H_2 and trace of B.[46] Furthermore, it has been predicted that MBHs containing Zn, such as $LiZn_2(BH_4)_5$, decompose by emitting diborane as main product.[47] Accordingly, to model the decomposition of pure and mixed MBHs, we consider the two following decomposition reactions:

$$Mg_{(1-x)}Zn_x(BH_4)_2 \rightarrow (1-x)MgH_{2(s)} + xZn_{(s)} + 2B_{(s)} + (3+x)H_{2(g)} \tag{5}$$

$$Mg_{(1-x)}Zn_x(BH_4)_2 \rightarrow (1-x)MgH_{2(s)} + xZn_{(s)} + B_2H_{6(g)} + xH_{2(g)} \tag{6}$$

In order to obtain the heat of reaction (ΔH_{dec}), the enthalpy for each product has been calculated (see Supporting Information for details about structure and energy). Figure 6 shows the computed enthalpy of decomposition for each solid solution as a function of Zn molar fraction for both reactions. The values are reported in kJ/mol instead of kJ/mol_{H2} in order to compare the two reaction paths and discriminate the stability difference for the

17

two sets of products. The limit values correspond to the decomposition of pure $Mg(BH_4)_2$ and $Zn(BH_4)_2$, respectively. As regards the Eq. 5, the result obtained for $Mg(BH_4)_2$ ($x = 0$) is about 125 kJ/mol, i.e. 42 kJ/mol_{H_2}, in good agreement with the value of 44 kJ/mol_{H_2} calculated by Setten and co-workers.[48] On the other hand, present results confirm that, at room temperature, $Zn(BH_4)_2$ ($x = 1$) is metastable and decomposes very easily, with a nearly zero enthalpy of reaction, in agreement with experimental evidence.[46] These results validate our computational approach, thus supporting our estimate of ΔH_{dec} for the Mg/Zn compounds. Computed decomposition enthalpies for the two reactions show a similar trend. The increase of zinc in the solid solution leads to a linear decrease of ΔH_{dec} with the production of B_2H_6 and H_2 being more endothermic than the formation of B and H_2 by a constant amount of 25 kJ/mol. According to experimental works[22,23], the decomposition of the mixed
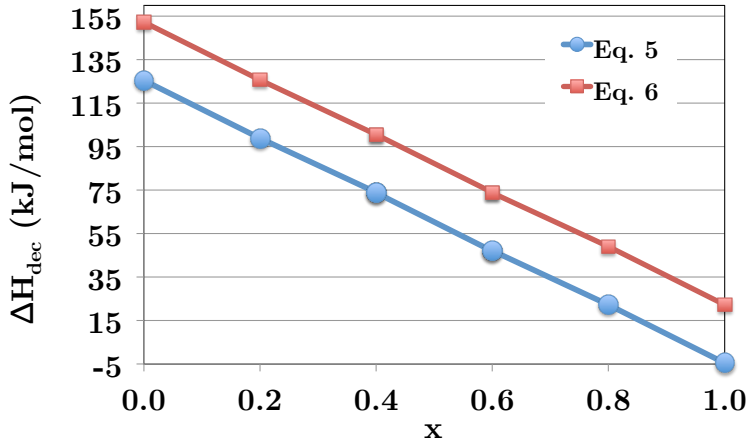

Figure 6: Decomposition enthalpy (kJ/mol) of the compounds for different molar fractions x of zinc, according to Eq.5.

Mg/Zn borohydride leads to the formation of a very small amount of B_2H_6. We can then refer to reaction 5 as the favored decomposition pathway. It turns out that for such reaction a molar fraction of Zn around 0.2-0.3 leads to the formation of a mixed Mg/Zn MBHs which decomposes with a ΔH_{dec} of about 85-95 kJ/mol. This corresponds to a value of 30 kJ/mol_{H_2} which is very close to the target decomposition enthalpy. Interestingly, a mixed $Mg_{(1-x)}Zn_x(BH_4)_2$ borohydride with x=0.1 has been synthesized[23] that shows a very low

decomposition temperature with respect to pure $Mg(BH_4)_2$, thus confirming the validity of our prediction.

Summary and Conclusions

The pure and mixed Mg/Zn borohydrides have been investigated by means of ab initio periodic DFT calculations. Computed free energies for the reaction of formation of Mg/Zn solid solutions, from $Mg(BH_4)_2$ and $ZnCl_2$, show that the synthesis may occurs spontaneously above room temperature. The enthalpy of decomposition of the mixed systems has then been computed by considering the formation of both B_2H_6 or B and H_2, along with MgH_2 and Zn. In the case of the decomposition reaction to B and H_2, we predicted that for a $Mg_{(1-x)}Zn_x(BH_4)_2$ borohydride, with a molar concentration of Zn of about 0.2, the ΔH_{dec} is close the value of interest (≈ 30 kJ/mol$_{H_2}$) for hydrogen sorption in mild conditions, in agreement with experimental findings[22,23].

In conclusion, the presence of Zn destabilizes the $Mg(BH_4)_2$ structure, thus reducing its decomposition enthalpy. Overall, the charge density topological analysis has allowed us to highlight the role of Zn when included in $Mg(BH_4)_2$. On the one hand, it does not alter the chemical bonding and coordination of the alkali earth metal borohydride in agreement with previous work by Łodziana and van Setten[37] , thus favoring the formation of the solid solution. On the other hand, the ability of Zn^{2+} to form bonds with $[BH_4]^-$ units with a more covalent character destabilizes the mixed compound and decreases the decomposition enthalpy.

Acknowledgments

Initiative under the E.U. project SSH2S (grant agreement n. 25665).

Supporting Information Available:

Table S1 with optimized structures of auxiliary systems; Preliminary data snalysis; Table S2 with average bond lengths for all solid solutions; Table S3 gathers all data available on topological analysis of the charge density.

This material is available free of charge via the Internet at http://pubs.acs.org.

References

(1) Schlapbach, L.; Züttel, A. Hydrogen-Storage Materials for Mobile Applications. *Nature* **2001**, *414*, 353–358.

(2) Felderhoff, M.; Weidenthaler, C.; von Helmolt, R.; Eberle, U. Hydrogen Storage: The Remaining Scientific and Technological Challenges. *Phys. Chem. Chem. Phys.* **2007**, *9*, 2643–2653.

(3) Targets for Onboard Hydrogen Storage Systems for Light-Duty Vehicles, 4.0. US Department of Energy, 2009; http://www1.eere.energy.gov/hydrogenandfuelcells/storage/current_technology.html.

(4) Materials Roadmap Enabling Low Carbon Energy Technologies. EU Commission staff working pager, 2011; http://ec.europa.eu/research/industrial_technologies/pdf/materials-roadmap-elcet-13122011_en.pdf.

(5) Chłopek, K.; Frommen, C.; Łeon, A.; Zabara, O.; Fichtner, M. Synthesis and Properties of Magnesium Tetrahydroborate, $Mg(BH_4)_2$. *J. Mater. Chem.* **2007**, *17*, 3496–3503.

(6) Filinchuk, Y.; Chernyshov, D.; Dmitriev, V. Light Metal Borohydrides: Crystal Structures and Beyond. *Z. Kristallogr.* **2008**, *223*, 649– 659.

(7) Meisner, G. P.; Scullin, M. L.; Balogh, M. P.; Pinkerton, F. E.; Meyer, M. S. Hydrogen Release from Mixtures of Lithium Borohydride and Lithium Amide: A Phase Diagram Study. *J. Phys. Chem. B.* **2006**, *110*, 4186–4192.

(8) Soloveichik, G.; Her, J.-H.; Stephens, P. W.; Gao, Y.; Rijssenbeek, J.; Andrus, M.; Zhao, J.-C. Ammine Magnesium Borohydride Complex as a New Material for Hydrogen Storage: Structure and Properties of $Mg(BH_4)_2 \cdot 2NH_3$. *Inorg. Chem.* **2008**, *47*, 4290–4298.

(9) Filinchuk, Y.; Hagemann, H. Structure and Properties of $NaBH_4 \cdot 2H_2O$ and $NaBH_4$. *Eur. J. Inorg. Chem.* **2008**, 3127–3133.

(10) Arnbjerg, L. M.; Ravnsbæk, D. B.; Filinchuk, Y.; Vang, R. T.; Cerenius, Y.; Besenbacher, F.; Jørgensen, J.-E.; Jakobsen, H. J.; Jensen, T. R. Structure and Dynamics for $LiBH_4$-$LiCl$ Solid Solutions. *Chem. Mater.* **2009**, *21*, 5772–5782.

(11) Zavorotynska, O.; Corno, M.; Damin, A.; Spoto, G.; Ugliengo, P.; Baricco, M. Vibrational Properties of MBH_4 and MBF_4 Crystals (M = Li, Na, K): A Combined DFT, Infrared, and Raman Study. *J. Phys. Chem. C* **2011**, *115*, 18890–18900.

(12) Nickels, E. A.; Jones, M. O.; David, W. I. F.; Johnson, S. R.; Lowton, R. L.; Sommariva, M.; Edwards, P. P. Tuning the Decomposition Temperature in Complex Hydrides: Synthesis of a Mixed Alkali Metal Borohydride. *Angew. Chem. Int. Ed* **2008**, *47*, 2817–2819.

(13) Hagemann, H.; Longhini, M.; Kaminski, J. W.; Wesolowski, T. A.; Černý, R.; Penin, N.; Sørby, M. H.; Hauback, B. C.; Severa, G.; Jensen, C. M. $LiSc(BH_4)_4$: A Novel Salt of Li^+ and Discrete $Sc(BH_4)_4{}^-$ Complex Anions. *J. Phys. Chem. A* **2008**, *112*, 7551–7555.

(14) Černý, R.; Ravnsbaek, D.; Severa, G.; Filinchuk, Y.; D'Anna, V.; Hagemann, H.; Haase, D.; Skibsted, J.; Jensen, C. M.; Jensen, T. R. Structure and Characterization of $KSc(BH_4)_4$. *J. Phys. Chem. C* **2010**, *114*, 19540–19549.

(15) Aidhy, D.; Wolverton, C. First-Principles Prediction of Phase Stability and Crystal Structures in Li-Zn and Na-Zn Mixed-Metal Borohydrides. *Phys. Rev. B* **2011**, *83*, 144111.

(16) Fang, Z.-Z.; Kang, X.-D.; Luo, J.-H.; Wang, P.; Li, H.-W.; Orimo, S. Formation and Hydrogen Storage Properties of Dual-Cation (Li, Ca) Borohydride. *J. Phys. Chem. C* **2010**, *114*, 22736–22741.

(17) Huan, T. D.; Amsler, M.; Sabatini, R.; Tuoc, V. N.; Le, N. B.; Woods, L. M.; Marzari, N.; Goedecker, S. Thermodynamic Stability of Alkali-Metal-Zinc Double-Cation Borohydrides at Low Temperatures. *Phys. Rev. B* **2013**, *88*, 024108.

(18) Ravnsbaek, D.; Filinchuk, Y.; Cerenius, Y.; Jakobsen, H.; Besenbacher, F.; Skibsted, J.; Jensen, T. A Series of Mixed-Metal Borohydrides. *Angew. Chem. Int. Ed.* **2009**, *48*, 6659–6663.

(19) Huan, T. D.; Amsler, M.; Tuoc, V. N.; Willand, A.; Goedecker, S. Low-Energy Structures of Zinc Borohydride $Zn(BH_4)_2$. *Phys. Rev. B* **2012**, *86*, 224110.

(20) Nakamori, Y.; Miwa, K.; Ninomiya, A.; Li, H.; Ohba, N.; Towata, S.; Züttel, A.; Orimo, S. Correlation Between Thermodynamical Stabilities of Metal Borohydrides and Cation Electronegativites: First-Principles Calculations and Experiments. *Phys. Rev. B* **2006**, *74*, 045126.

(21) Hummelshøj, J. S.; Landis, D. D.; Voss, J.; Jiang, T.; Tekin, A.; Bork, N.; Dułak, M.; Mortensen, J. J.; Adamska, L.; Andersin, J.; et. al, Density Functional Theory Based Screening of Ternary Alkali-Transition Metal Borohydrides: A Computational Material Design Project. *J. Chem. Phys.* **2009**, *131*, 014101.

(22) Albanese, E.; Kalantzopoulos, G.; Vitillo, J.; Pinatel, E.; Civalleri, B.; Deledda, S.; Bordiga, S.; Hauback, B.; Baricco, M. Theoretical and Experimental Study on $Mg(BH_4)_2$-$Zn(BH_4)_2$ Mixed Borohydrides. *J. Alloys Compd.* **2013**, *580*, S282 – S286.

(23) Kalantzopoulos, G. N.; Vitillo, J. G.; Albanese, E.; Pinatel, E.; Civalleri, B.; Deledda, S.; Bordiga, S.; Baricco, M.; Hauback, B. C. Hydrogen Storage of Mg-Zn Mixed Metal Borohydrides. *J. Alloys and Compd.* **2013**, *doi 10.1016/j.jallcom.2013.12.258*.

(24) Perdew, J. P.; Burke, K.; Ernzerhof, M. Generalized Gradient Approximation Made Simple. *Phys. Rev. Lett.* **1996**, *77*, 3865–3868.

(25) Dovesi, R.; Sauders, V. R.; Roetti, C.; Orlando, R.; Zicovich-Wilson, C. M.; Pascale, F.; Civalleri, B.; Doll, K.; Harrison, N. M.; et al., I. J. B. *CRYSTAL09* **2009**, *University of Torino, Torino*.

(26) Dovesi, R.; Orlando, R.; Civalleri, B.; Roetti, C.; Saunders, V. R.; Zicovich-Wilson, C. M. CRYSTAL: A Computational Tool for the *ab initio* Study of the Electronic Properties of Crystals. *Z. Kristallogr.* **2005**, *220*, 571–573.

(27) Weigend, F.; Ahlrichs, R. Balanced Basis Sets of Split Valence, Triple Zeta Valence and Quadruple Zeta Valence Quality for H to Rn: Design and Assessment of Accuracy. *Phys. Chem. Chem. Phys.* **2005**, *7*, 3297–3305.

(28) Pascale, F.; Zicovich-Wilson, C. M.; Gejo, F. L.; Civalleri, B.; Orlando, R.; Dovesi, R. The Calculation of the Vibrational Frequencies of Crystalline Compounds and its Implementation in the CRYSTAL Code. *J. Comput. Chem.* **2004**, *25*, 888–897.

(29) Zicovich-Wilson, C. M.; Torres, F. J.; Pascale, F.; Valenzano, L.; Orlando, R.; Dovesi, R. Ab initio Simulation of the IR Spectra of Pyrope, Grossular, and Andradite. *J. Comput. Chem.* **2008**, *29*, 2268–2278.

(30) Gatti, C.; Saunders, V. R.; Roetti, C. Crystal Field Effects on the Topological Properties of the Electron Density in Molecular Crystals: The Case of Urea. *J. Chem. Phys.* **1994**, *101*, 10686–10696.

(31) Gatti, C.; Casassa, S. TOPOND User's Manual. CNR-ISTM: Milano, Italy, 2014.

(32) Bader, R. F. W.; Essén, H. The Characterization of Atomic Interactions. *J. Chem. Phys.* **1984**, *80*, 1943–1960.

(33) Gatti, C. Chemical Bonding in Crystals: New Directions. *Z. Kristallogr.* **2005**, *220*, 399–457.

(34) Černý, R.; Filinchuk, Y.; Hagemann, H.; Yvon, K. Magnesium Borohydride: Synthesis and Crystal Structure. *Angew. Chem., Int. Ed. 46,* **2007**, *46*, 5765–5767.

(35) Her, J. H.; Stephens, P. W.; Gao, Y.; Soloveichik, G. L.; Rijssenbeek, J.; Andrus, M.; Zhao, J. C. Structure of Unsolvated Magnesium Borohydride $Mg(BH_4)_2$. *Acta Crystallographica* **2007**, *Section B 63*, 561–568.

(36) Filinchuk, Y.; Černý, R.; Hagemann, H. Insight into $Mg(BH_4)_2$ with Synchrotron X-ray Diffraction: Structure Revision, Crystal Chemistry, and Anomalous Thermal Expansion. *Chem. Mater.* **2009**, *21*, 925–933.

(37) Łodziana, Z.; van Setten, M. J. Binding in Alkali and Alkaline-Earth Tetrahydroborates: Special Position of Magnesium Tetrahydroborate. *Phys. Rev. B* **2010**, *81*, 024117.

(38) Filinchuk, Y.; Richter, B.; Jensen, T. R.; Dmitriev, V.; Chernyshov, D.; Hagemann, H. Porous and Dense Magnesium Borohydride Frameworks: Synthesis, Stability, and Reversible Absorption of Guest Species. *Angew. Chem., Int. Ed.* **2011**, *50*, 11162–11166.

(39) Espinosa, E.; Alkorta, I.; Elguero, J.; Molins, E. From Weak to Strong Interactions: A Comprehensive Analysis of the Topological and Energetic Properties of the Electron Density Distribution Involving X-H⋯F-Y Systems. *J. Chem. Phys.* **2002**, *117*, 5529–5542.

(40) Gervasio, G.; Bianchi, R.; Marabello, D. About the Topological Classification of the Metal-Metal Bond. *Chem. Phys. Lett.* **2004**, *387*, 481–484.

(41) http://webbook.nist.gov/chemistry/.

(42) Voss, J.; Hummelshøj, J.; Łodziana, Z.; Vegge, T. Structural Stability and Decomposition of $Mg(BH_4)_2$ Isomorphs-an *ab initio* Free Energy Study. *J. Phys. Condens. Matter* **2009**, *21*, 012203.

(43) Zhang, Y.; Majzoub, E.; Ozoliņš, V.; Wolverton, C. Theoretical Prediction of Different Decomposition Paths for $Ca(BH_4)_2$ and $Mg(BH_4)_2$. *Phys. Rev. B* **2010**, *82*, 174107.

(44) Chong, M.; Karkamkar, A.; Autrey, T.; Orimo, S.; Jalisatgid, S.; Jensen, C. M. Reversible Dehydrogenation of Magnesium Borohydride to Magnesium Triborane in the Solid State Under Moderate Conditions. *Chem. Commun.* **2011**, *47*, 1330–1332.

(45) Paskevicius, M.; Pitt, M. P.; Webb, C. J.; Sheppard, D. A.; Filsø, U.; Gray, E. M. A.; Buckley, C. E. In-Situ X-ray Diffraction Study of γ-$Mg(BH_4)_2$ Decomposition. *J. Phys. Chem. C* **2012**, *116*, 15231–15240.

(46) Jeon, E.; Cho, Y. Mechanochemical Synthesis and Thermal Decomposition of Zinc Borohydride. *J. Alloys Comp.* **2006**, *422*, 273–275.

(47) Borgschulte, A.; Callini, E.; Probst, B.; Jain, A.; Kato, S.; Friedrichs, O.; Remhof, A.; Bielmann, M.; Ramirez-Cuesta, A. J.; Züttel, A. Impurity Gas Analysis of the Decomposition of Complex Hydrides. *J. Phys. Chem. C* **2011**, *115*, 17220–17226.

(48) Setten, M. J. V.; Wijs, G. A. D.; Fichtner, M.; Brocks, G. A Density Functional Study of α-$Mg(BH_4)_2$. *Chem. Mater.* **2008**, *20*, 4952–4956.

Graphical TOC Entry